Title

An examination of the role of particles in oceanic mercury cycling

Journal

Philosophical Transactions of the Royal Society A Mathematical Physical and Engineering Sciences, 374(2081)

ISSN

1364-503X

Authors

Lamborg, Carl H
Hammerschmidt, Chad R
Bowman, Katlin L

Publication Date

2016-11-28

DOI

10.1098/rsta.2015.0297

Peer reviewed

PHILOSOPHICAL TRANSACTIONS A

rsta.royalsocietypublishing.org

Research

Cite this article: Lamborg CH, Hammerschmidt CR, Bowman KL. 2016 An examination of the role of particles in oceanic mercury cycling. *Phil. Trans. R. Soc. A* **374**: 20150297.
http://dx.doi.org/10.1098/rsta.2015.0297

Accepted: 20 July 2016

One contribution of 20 to a discussion meeting issue 'Biological and climatic impacts of ocean trace element chemistry'.

Subject Areas:
geochemistry, oceanography

Keywords:
mercury, ocean particles, biological pump

Author for correspondence:
Carl H. Lamborg
e-mail: clamborg@ucsc.edu

An examination of the role of particles in oceanic mercury cycling

Carl H. Lamborg[1], Chad R. Hammerschmidt[2] and Katlin L. Bowman[1]

[1]Department of Ocean Sciences, University of California, Santa Cruz, CA 95064, USA
[2]Department of Earth and Environmental Sciences, Wright State University, Dayton, OH 45435, USA

CHL, 0000-0003-4379-3904

Recent models of global mercury (Hg) cycling have identified the downward flux of sinking particles in the ocean as a prominent Hg removal process from the ocean. At least one of these models estimates the amount of anthropogenic Hg in the ocean to be about 400 Mmol, with deep water formation and sinking fluxes representing the largest vectors by which pollutant Hg is able to penetrate the ocean interior. Using data from recent cruises to the Atlantic, we examined the dissolved and particulate partitioning of Hg in the oceanic water column as a cross-check on the hypothesis that sinking particle fluxes are important. Interestingly, these new data suggest particle-dissolved partitioning (K_d) that is approximately 20× greater than previous estimates, which thereby challenges certain assumptions about the scavenging and active partitioning of Hg in the ocean used in earlier models. For example, the new particle data suggest that regenerative scavenging is the most likely mechanism by which the association of Hg and particles occurs.

This article is part of the themed issue 'Biological and climatic impacts of ocean trace element chemistry'.

1. Introduction

As with other trace metals in the ocean, mercury (Hg) can be found both in solution and associated with particles. The distribution between these two phases exerts a primary control on the residence time of Hg

THE ROYAL SOCIETY PUBLISHING

in the ocean, as it does with other metals, because the particulate phase facilitates the slow, downward flux of Hg to the seafloor. A greater affinity of metals to particles could facilitate faster removal from the oceanic water column and lower concentrations in seawater.

Sinking and suspended particles are also locations of enhanced microbial activity and, therefore, of special interest for understanding the biogeochemical transformations of Hg. These transformations include reduction of Hg^{2+} to Hg^0 and methylation of Hg^{2+} to CH_3Hg^+ and $(CH_3)_2Hg$. Elemental Hg is a dissolved gas present in the ocean at high degrees of supersaturation and, therefore, drives a net evasion of Hg to the atmosphere, 'detoxifying' the ocean. Methylation reactions, by contrast, produce highly bioaccumulative organo-Hg compounds, CH_3Hg^+ and $(CH_3)_2Hg$, that are at the heart of human and environmental health risks related to Hg. Each of these transformations can be biologically mediated [1,2], suggesting that Hg reduction and methylation may be enhanced in particles because they are sites of increased microbial activity (e.g. [3]).

Particles themselves are not static, however, and slowly degrade as they sink, which lowers the mass and flux of trace metals to sediments. The loss of particulate mass and flux with increasing depth does not completely eliminate the ocean's ability to remove Hg from shallow parts of the water column. Instead, particle flux acts as a pump to move Hg from shallow parts of the ocean to greater depths and thereby store Hg away from most organisms for centuries to millennia. This so-called biological pump behaves in complex ways with dependencies that include productivity in surface water, the coupling of producer and consumer organisms, subsurface microbial communities, and water temperature and circulation [4–7], each of which are the subject of much current research.

In the case of Hg, the biological pump mitigates the amount of anthropogenic Hg residing in the surface ocean. Humans have severely perturbed the natural Hg cycle, with estimates ranging from 3 to 7 times more Hg moving among the active reservoirs of the Earth today (the Anthropocene) than in the Holocene before human influence was noticeable [8]. Thus, a central challenge in current global-scale Hg biogeochemical research is to understand the fate of this pollution Hg and especially its amount and location in the ocean. Recently, two groups making use of new as well as established datasets of Hg concentrations and speciation in the ocean came to essentially the same conclusion that (i) about 400 Mmol of anthropogenic Hg currently resides in the ocean, (ii) the deep North Atlantic is a notable location of current pollution Hg storage (approx. 25% of total), and (iii) the surface ocean has been perturbed by about 3.5–4.4× compared with the pre-industrial period [9,10]. The techniques used by the two groups were somewhat indirect in their approaches and require further validation and cross-checking to ensure they represent a sound interpretation of the data. One important way to further test these hypotheses is by examining particulate Hg dynamics in the ocean. A refined understanding of these dynamics will improve the predictive power of ocean Hg models and allow for a better understanding of the fate of pollutant Hg that currently resides in the ocean as well as gauge the limits to which humans can continue to perturb the cycle.

For these reasons, a greater understanding of the cycling and fate of particulate Hg in the ocean is needed, and some studies have already turned attention to this issue [9,11,12]. Most modelling efforts have assumed that Hg partitions between the dissolved and particle phases in a dynamic way (both sorption and desorption) that can be modelled well by assuming equilibrium. With natural particles, equilibrium partitioning is frequently estimated with a partition coefficient, or K_d, which is the particle Hg concentration divided by the solution-phase concentration. The particle-phase concentration is most often normalized to some measure of either particle abundance or influence, such as total mass, surface area or the mass of a certain component of the particles (e.g. lithogenic material). In the case of Hg, and in the light of the observation that Hg exhibits strong associations with organic matter under a variety of situations [13], the K_d value used in most modelling exercises is one that has been normalized to, or corrected for, the organic carbon content of either sinking or suspended particles. Furthermore, due to a relative lack of appropriate data, K_d values are often assumed to be constant with depth in the open ocean and uniform within and among ocean basins, although coastal systems are different, as

discussed below. While the assumption of partitioning homogeneity is reasonable, it has not been extensively tested, especially under open-ocean conditions.

The on-going international GEOTRACES programme is providing new and large datasets of particle and dissolved Hg concentrations and speciation as well as particle geochemistry, in general. Here, we use results from a recent US GEOTRACES zonal transect of the North Atlantic Ocean (GA03) to test some of the underlying assumptions behind our understanding of Hg particle dynamics.

2. Data and models

Details of water and particle sampling during the GA03 cruise have been described in detail elsewhere [14–16]. In brief, water samples for dissolved Hg (i.e. less than 0.2 µm) were recovered from 27 stations extending nearly zonally across the North Atlantic from Woods Hole, MA, USA, to the Cape Verde Islands (sampled in 2011), and into the Mauritanian upwelling along West Africa (sampled in 2010). Additionally, we completed a relatively short meridional section from Lisbon, Portugal to the Cape Verde Islands, but we do not include those data in this discussion for simplicity. At each sampling station, as many as 24 depths were sampled with a trace metal clean rosette [17], and surface water (approx. 2 m depth) was collected with an underway 'towed fish' [18]. Water was filtered to 0.2 µm promptly after sampling, and in the case of total Hg in filtered water, all analyses were performed on-board the ship within 48 h of sampling.

Particulates were collected onto quartz-fibre filters by *in situ*, battery-operated pumps that were hung from a non-metallic wire [15] at 22 stations along the same transect and at a maximum of 18 depths per station. Particle sampling depths were nominally the same as some of those sampled for the dissolved phase. Filters were processed on board the vessel promptly after sampling, including obtaining discrete subsamples (i.e. 'punches') that were stored frozen until analysis of total Hg on shore.

The compositions of the particles (i.e. amounts of organic matter, $CaCO_3$, biogenic opal, detrital lithogenic material, authigenic Fe hydroxide and Mn oxide minerals) were determined on other subsamples by Dr Phoebe Lam and colleagues, and total mass of particles was estimated as the sum of these phases [15]. While two size classes of particles were collected using these systems, limitations in the amount of material collected from the large size class (greater than 51 µm) meant that only small-sized particles (1–51 µm) were available for Hg analyses. This size class is generally viewed as non-sinking (i.e. suspended particulate matter, SPM), while the larger size class is used to estimate the composition of the sinking pool of particulate matter. We can estimate the contribution of the larger size class to the total particulate Hg pool based on (i) the observation that the larger sized particle mass along this transect was about 22% of the total mass [15] and (ii) using the Hg/SPM of the larger size class measured from other cruises. For example, Munson *et al.* [19] collected sinking particles in the tropical Pacific and found Hg/SPM ratios around 10^{-3} µmol g^{-1}, which is quite a bit less than the ratios reported here for the suspended size fraction. Thus, Hg associated with sinking-sized particles probably represents a small fraction of all particulate Hg along this transect, justifying our view that the 'suspended' pool can be used as a proxy for the bulk particle pool.

3. Water column trends

Profiles of particulate Hg, at each of the stations where *in situ* pumping was performed, are shown in figure 1 as both un-normalized concentration (picomoles of particulate Hg per litre of seawater) as well as concentrations normalized to the amount of total SPM (micrograms per litre) and POC (micrograms per litre). The un-normalized concentrations were already summarized by Bowman *et al.* [14], and we show them again here to compare with normalized values. Non-normalized particulate Hg concentrations generally decrease with depth at each station, and are broadly consistent with assessments that the vertical distribution of particulate Hg follows that of POC

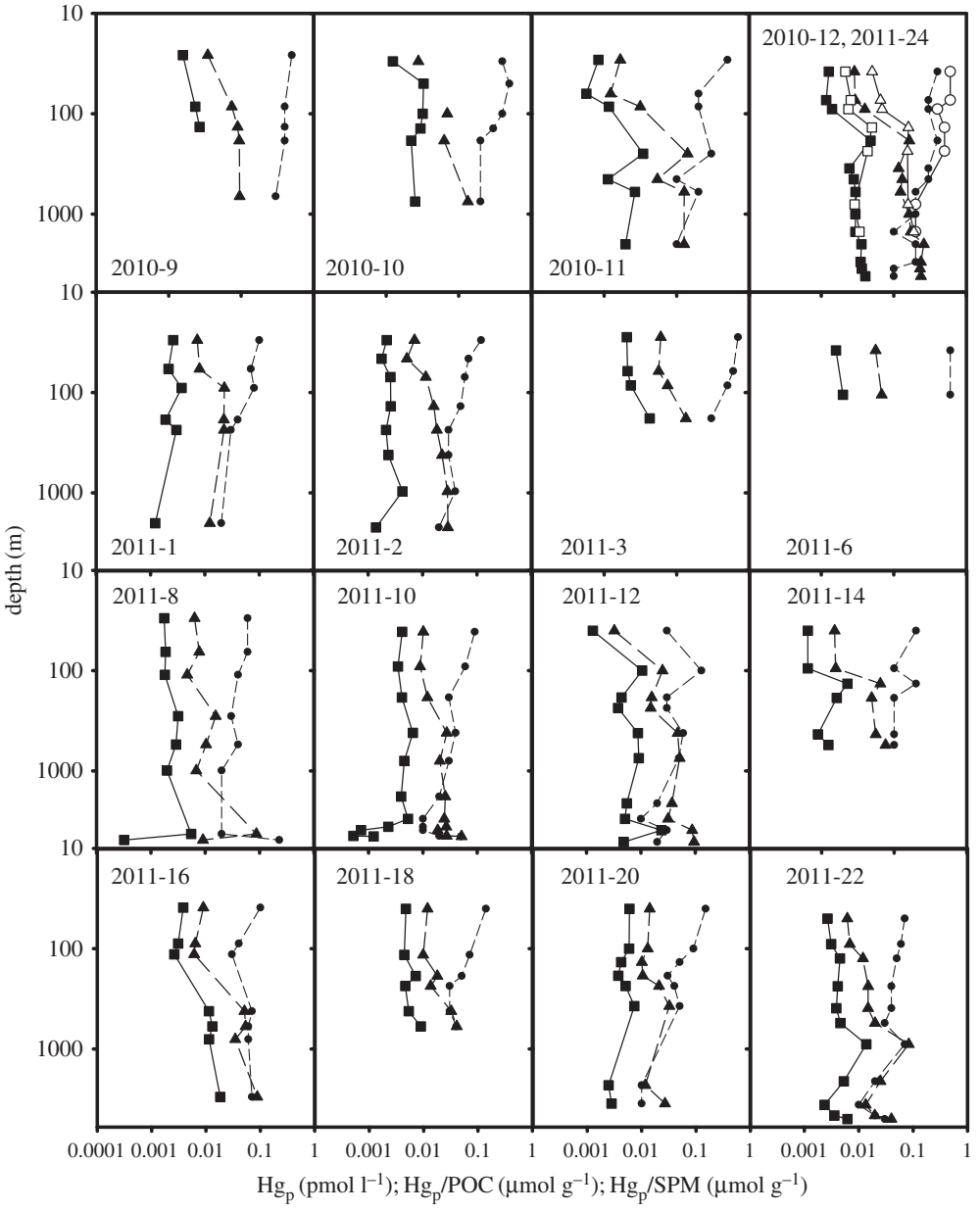

Figure 1. Vertical distributions of particulate Hg at stations during US GEOTRACES cruise GA03. Each panel represents the results from a single station. Particulate Hg (circles), POC-normalized particulate Hg (triangles) and SPM-normalized particulate Hg (squares). Results for stations 2010-12 and 2011-24 are shown together as they represent samples from the same station occupied on both legs. Measurements associated with a hydrothermal plume at station 16 were not included.

in a 'Martin curve' power law-type function, often summarized as

$$C(z) = C_0\left(\frac{z}{z_0}\right)^b, \tag{3.1}$$

where $C(z)$ is the concentration of particulate Hg (pmol l^{-1}) at depth z, C_0 is the concentration at the reference depth z_0 (often taken as the bottom of the mixed layer, photic zone or 100 m; e.g. [4]), and b is the power law exponent. In a log–log plot, such as figure 1, a close correspondence to this

Table 1. The fitted C_0 and b values for particulate Hg from GA03. Values were determined from nonlinear least squares and a canonical z_0 value of 100 m. Stations 2010-12 and 2011-24 were the same location, sampled on both legs.

	Hg_{part} un-normalized			Hg_{part} POC-normalized			Hg_{part} SPM-normalized		
station	C_0 (pmol l^{-1})	b	r^2	C_0 (pmol μg^{-1})	b	r^2	C_0 (pmol μg^{-1})	b	r^2
2010-9	0.041	−0.14	0.94	0.0072	0.21	0.67	0.0022	0.11	0.50
2010-10	0.034	−0.27	0.67	0.0033	0.70	0.71	0.0025	0.05	0.04
2010-11	0.026	−0.36	0.60	0.0052	0.34	0.54	0.0014	0.19	0.24
2010-12	0.033	−0.22	0.71	0.0075	0.33	0.84	0.0021	0.17	0.46
2011-1	0.059	−0.45	0.90	0.0154	0.05	0.04	0.0025	−0.13	0.29
2011-2	0.058	−0.47	0.85	0.0130	0.30	0.89	0.0024	0.04	0.03
2011-3	0.045	−0.39	0.91	0.0091	0.58	0.87	0.0030	0.50	0.85
2011-6	n.a.	n.a.	n.a.	n.a.	n.a.	n.a.	n.a.	n.a.	n.a.
2011-8	0.026	0.40	0.21	0.0057	0.54	0.35	0.0021	0.08	0.06
2011-10	0.060	−0.35	0.72	0.0126	0.24	0.50	0.0044	−0.13	0.22
2011-12	0.057	−0.20	0.20	0.0158	0.41	0.68	0.0053	0.19	0.15
2011-14	0.015	−0.27	0.45	0.0034	0.45	0.65	0.0012	0.09	0.04
2011-16	0.062	0.00	0.00	0.0166	0.50	0.85	0.0052	0.39	0.88
2011-18	0.076	−0.65	0.95	0.0101	0.77	0.88	0.0050	0.22	0.40
2011-20	0.077	−0.72	0.93	0.0153	0.11	0.14	0.0054	−0.15	0.39
2011-22	0.057	−0.24	0.58	0.0165	0.18	0.12	0.0044	0.06	0.03
2011-24	0.049	−0.28	0.78	0.0097	0.26	0.69	0.0031	0.06	0.07

model would appear as a straight line. Martin and colleagues found that particulate carbon flux in the ocean (presumably proportional to particulate concentrations) followed such a functional form with a b-value of −0.858 for their composite of open-ocean data [20]. A few anomalous samples in a submarine hydrothermal plume (Station 2011-16) have been removed from the full Bowman *et al.* dataset for this analysis. Concentrations of particulate Hg measured in the plume were anomalously high and not representative of ordinary conditions. The b exponent for particulate Hg had a wide range of values among stations, from −0.72 to 0.40 with a mean of -0.29 ± 0.26 (table 1). Interestingly, particulate Hg therefore exhibited, in general, a less dramatic decrease in concentration with depth than does organic carbon (i.e. b exponents greater than −0.8). This suggests that Hg is not merely a passive passenger on oceanic particles. Otherwise, its vertical distribution would have a b exponent closer to that of particulate organic matter (POM).

At almost all stations, vertical distributions of mass- and organic carbon-normalized particulate Hg had b values greater than zero, indicating increasing Hg/POC and Hg/SPM ratios with depth. This suggests that the capacity of marine particles to sorb Hg is not saturated, which is not surprising given the low concentrations of Hg in seawater of the North Atlantic Ocean (0.1–2 pM [14]). Interestingly, b exponents for SPM-normalized particulate Hg (from −0.15 to 0.5; mean = 0.1) were closer to zero (and invariant with depth) than POC-normalized b exponents (0.05–0.77; mean = 0.4), indicating that SPM may be better at accounting for vertical distributions of Hg than is POC. This observation is in contrast with the assumption that organic carbon and associated ligands control Hg biogeochemistry in both the dissolved and particulate phases.

Another way to examine the distinction between organic matter and total mass in affecting Hg cycling is to examine vertical and horizontal variability of K_d normalized to total suspended mass (figure 2). The partition coefficients ranged about 100-fold among samples, from 2.6×10^5

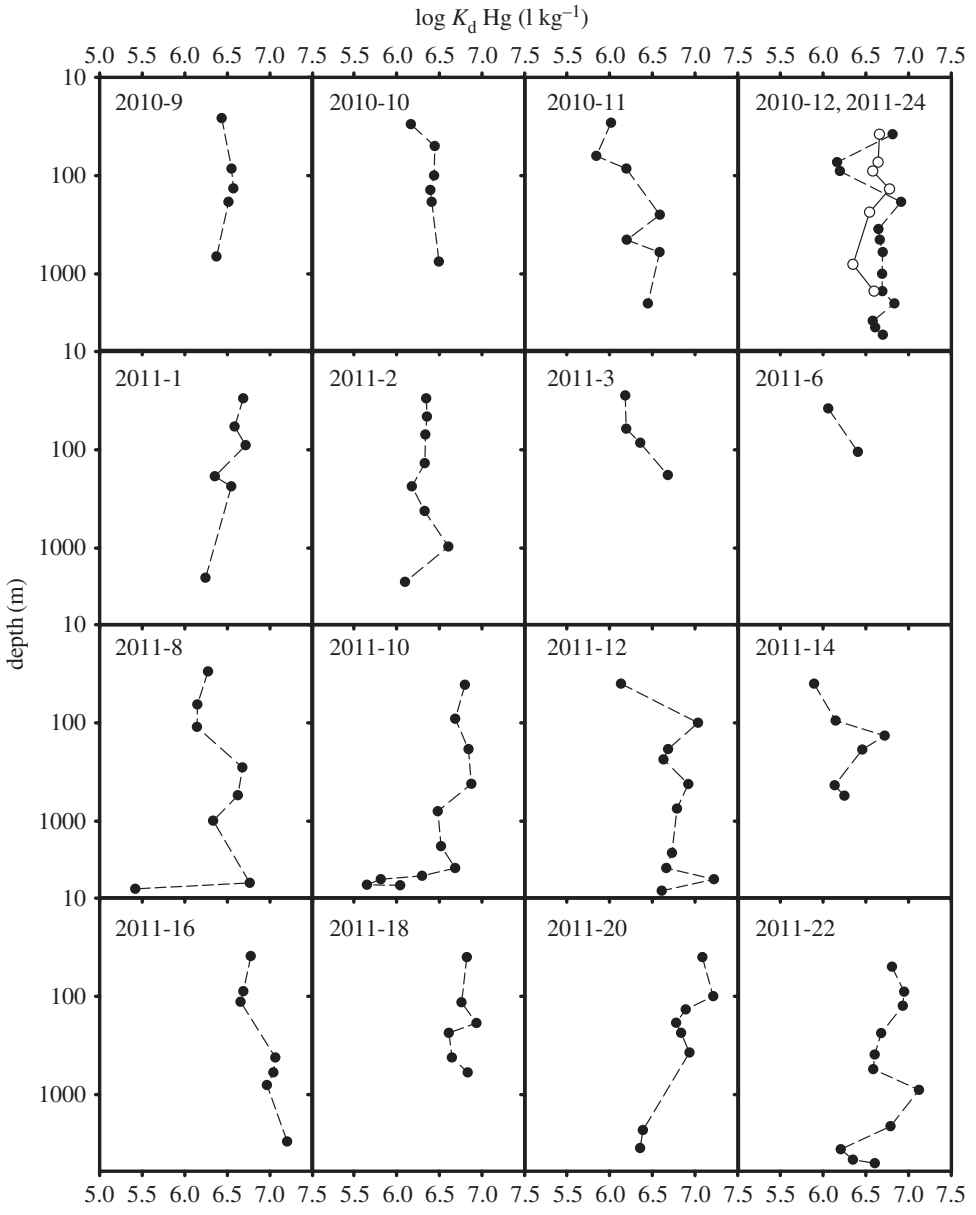

Figure 2. Station-by-station vertical profiles of Hg partitioning coefficients (K_d). The K_d value was calculated with particulate Hg normalized to the mass of suspended particulate matter. Results for stations 2010-12 and 2011-24 are shown together as they represent samples from the same station occupied on both legs. Measurements associated with a hydrothermal plume at station 16 were not included.

to 3.9×10^7 l kg^{-1}, with a mean value of $(4.5 \pm 3.1) \times 10^6$ l kg^{-1}. These K_d values rival those of quintessential 'particle-reactive' elements, such as Th [21]. At most stations, K_d values were relatively constant with depth, although there were examples of both increasing and decreasing values with depth. No significant trends were observed across the transect, even though there was a wide range of productivity and scavenging rates among stations as indicated by nutrients, thorium and particle distributions [15,22,23]. Thus, adoption of a single K_d value vertically and horizontally, at least within this basin, appears defensible. We also examined the K_d values for any evidence of a 'particle-concentration effect', wherein the apparent K_d value decreases

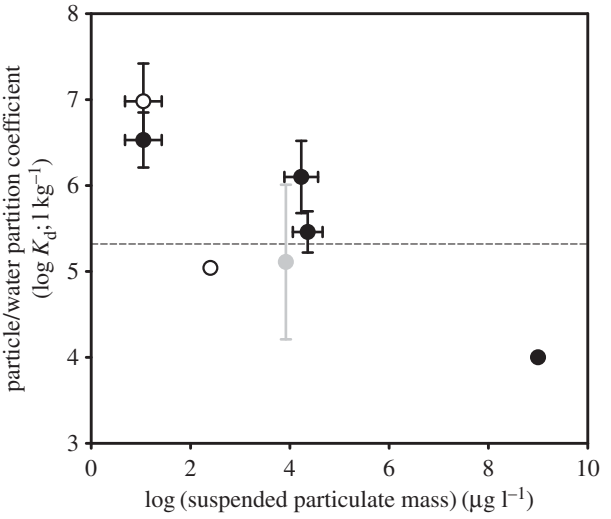

Figure 3. Mass-normalized partition coefficients (K_d) of Hg from a variety of marine and freshwater environments plotted against suspended mass concentration (from left to right: GA03 (this work); North Atlantic [12]; Connecticut River at Haddam, CT [24]; New York/New Jersey Harbour [25]; San Francisco Bay [26]; Continental Shelf porewater [27]). River data are denoted by the grey symbol, while the open symbols are K_d's calculated using just the concentration of dissolved Hg^{2+} rather than dissolved total Hg (black symbols). The dashed line is the value of K_d used by Zhang *et al.* in their models [9,28].

as suspended particulate mass increases. No inverse relationship between K_d and SPM was observed over the range of SPM determined on this cruise, unlike that for Th and Pa [21]. A potential, but weak, particle-concentration effect may exist for Hg in natural water, but only if other high particle-load conditions are considered. For example, figure 3 illustrates a compilation of K_d values from a variety of aquatic environments including coastal embayments, rivers and marine sediment porewaters that have high particle loads. The particle-concentration effect is fairly weak, with K_d of Hg dropping only about 2.5 orders of magnitude over an 8 order range in SPM, and comparable with that observed for Th and Pa [21].

Of particular interest is that the average K_d value observed during the cruise is about 21× greater than the value of 2.1×10^5 l kg^{-1} used by Zhang and colleagues to successfully model GEOTRACES Hg results and other data previously [9,28]. This begs the question of whether the K_d we observed during the cruise is still consistent with the assumption that Hg can be scavenged from the water column by particles in an equilibrium, reversible way and whether this sorption is controlled by organic matter. To test this hypothesis, we performed two modelling exercises. The first was a de-convolution similar to that presented by Hayes *et al.* [21]. The apparent phase-specific, intrinsic K_d values for each of the components of the bulk particulate as determined by Lam *et al.* [15] were calculated by performing a multiple linear regression of all bulk K_d values against the sample-by-sample fraction of total particulate mass in each phase. This was done using the non-negative least-squares function in Matlab (lsqnonneg) to force physically plausible values, and uncertainty was estimated as by Hayes *et al.* [21]. The phases included in the Lam *et al.* [15] calculations were POM (as traced by POC), $CaCO_3$ (as traced by particulate total carbon less the POC), lithogenic material (as traced by particulate Al), biogenic silica and authigenic MnO_2 and $Fe(OH)_3$ as traced by non-lithogenic Mn and Fe, respectively. Surprisingly, the phase exhibiting the highest apparent intrinsic K_d value was manganese oxide, followed closely by iron hydroxide (table 2). Neither of these phases has been demonstrated in previous marine Hg studies to be especially important in Hg sorption, and indeed their relative scarcity when compared with other phases in most environments implies that they are not likely to be dominant components of Hg sorption. However, we reported earlier [14] that particulate Hg

Table 2. Apparent intrinsic K_d values of Hg for each of the separate particulate phases, determined by non-negative least-squares fit. The K_d values were estimated from dissolved total Hg, rather than dissolved Hg(II). The relative standard deviation (r.s.d.) is the variability estimated for the intrinsic K_d values using the jackknifed resampling approach employed by Hayes *et al.* [21]. The typical contribution to mass by each fraction is the average value for particles below 100 m depth.

particulate fraction	intrinsic log K_d (l kg^{-1})	r.s.d. (%)	typical contribution to particle mass (%)
particulate organic matter	6.72	2	36 ± 18
lithogenic material	5.84	9	30 ± 19
$CaCO_3$	6.71	4	29 ± 11
biogenic silica	n.a.	n.a.	4 ± 3
iron hydroxides	7.64	9	0.8 ± 5
manganese oxides	8.29	16	0.1 ± 0.2

was enriched in the plume of the TAG hydrothermal vent field and speculated at that time that iron hydroxides might be the cause. The relatively high intrinsic K_d for Fe hydroxides suggested by this new examination would appear to support that hypothesis. Furthermore, these findings suggest that Hg sorption to authigenic mineral phases in other circumstances (e.g. porewaters and aquifers) should be considered more carefully. For example, Johannesson & Neuman [29] recently suggested a prominent role of iron hydroxide coatings for sorbing Hg in a confined aquifer, and our results here may support their conclusions. Of the phases that comprise the majority of particulate mass, POM and $CaCO_3$ had the largest intrinsic K_d values and were nearly equal. This is consistent with our observation that Hg has a better correlation to total particulate mass than just POM. It remains to be tested whether this implies that Hg is inherently 'sticky' to $CaCO_3$ or instead to some residual organic fraction that remains protected from degradation by carbonates. The net result, however, is that Hg apparently can be pumped more deeply into the water column than modelling with sorption just to POM would suggest. It also suggests that regions/times when sinking particle mass is dominated by biogenic silica, for example, following diatom blooms, may not be as effective at removing Hg from surface waters as other conditions as that phase showed little affinity for Hg in this analysis. We must consider, however, that this dataset has relatively low particulate silica compared with locations such as the Southern Ocean, and that this statistical approach to understanding Hg sorption offers apparent K_d values for various phases. True sorption of Hg to biogenic silica could very well be significant in other ocean regions and should be investigated in laboratory studies along with other marine particle phases.

Our second modelling exercise was an inversion meant to extract apparent rate constants for Hg partitioning with particles from vertical profiles of dissolved and particulate Hg as well as particulate mass. Partitioning dynamics in the model included sorption of dissolved Hg to particles, desorption of particulate Hg to the dissolved pool, remineralization of particles forcing particulate components into the solution phase, sinking of particles and diffusion in the dissolved phase (figure 4). These dynamics are similar to those used in other studies (e.g. [30–33]), and governed by the following equations:

$$\frac{\partial[D]}{\partial t} = (k_{\mathrm{rem}} + k_{\mathrm{dsb}})[P] - k_{\mathrm{ads}}[\mathrm{SPM}][D] + \kappa \frac{\partial^2[D]}{\partial z^2} \tag{3.2}$$

and

$$\frac{\partial[P]}{\partial t} = -(k_{\mathrm{rem}} + k_{\mathrm{dsb}})[P] + k_{\mathrm{ads}}[\mathrm{SPM}][D] - w\frac{\partial[P]}{\partial z}. \tag{3.3}$$

Sinking rate (w) was assumed constant with depth (2 m d^{-1}, taken from Th modelling by Anderson *et al.* in this issue and appropriately slow given we are dealing with the suspended pool as a proxy for all particles) as was the vertical diffusivity, κ, at 10^{-5} m^2 s^{-1} [34,35]. The

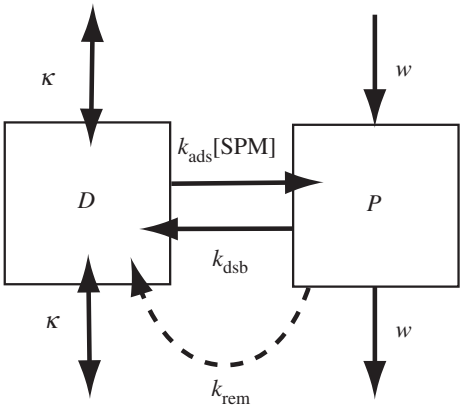

Figure 4. Our particle dynamics model, adapted from Marchal & Lam [30]. The dissolved (*D*) and particle (*P*) pools are connected by adsorption, desorption and remineralization. Vertical transport of the two pools is facilitated by sinking of particles and diffusion of dissolved Hg.

value of k_{rem} was derived by assuming the change in particle mass flux with depth was balanced by remineralization:

$$w\frac{\Delta[\mathrm{SPM}]}{\Delta z} = k_{rem}[\mathrm{SPM}]. \tag{3.4}$$

The value of k_{rem} was calculated for each depth for each station, and a station-by-station average was calculated. Because k_{rem} is calculated based solely on mass, it represents the conversion of particulate Hg to dissolved Hg associated with all particle phases. As Hg appears associated with the two phases (organic matter and calcium carbonate) whose remineralization from the particle phase constitutes most of the sinking mass flux loss, this is a reasonable simplification to make at this stage of our investigation. A non-uniform k_{rem} approach also was tried, but it occasionally generated nonsensical negative k_{rem} values that, at this level of modelling, could not be interpreted. Finally, we performed station-by-station inversions of the following finite difference matrix, with two rows per depth, yielding depth-specific least-square fits for k_{ads} and k_{dsb}:

$$\begin{bmatrix} \cdots & \\ -[\mathrm{SPM}][D]_i & [P]_i \\ [\mathrm{SPM}][D]_i & -[P]_i \\ \cdots & \end{bmatrix} \begin{bmatrix} k_{ads} \\ k_{dsb} \end{bmatrix} = \begin{bmatrix} \cdots \\ -k_{rem}[P]_i - \dfrac{\kappa([D]_{i-1} - 2[D]_i + [D]_{i+1})}{\Delta z^2} \\ k_{rem}[P]_i + \dfrac{w([P]_{i-1} - [P]_i)}{\Delta z} \\ \cdots \end{bmatrix}. \tag{3.5}$$

At about two-thirds of all depths sampled below the nominal mixed layer depth of 100 m (figure 5), apparent k_{dsb} values were zero and/or well below the value for k_{rem} suggesting that Hg particle dynamics were essentially a balance between adsorption from the dissolved phase and remineralization to the dissolved phase. This is closer to the 'regenerative scavenging' dynamic that John & Conway [34] observed for Zn cycling, which fit better than the reversible scavenging-like dynamic of Bacon & Anderson [32].

We further examined the inversion-derived rate constants by calculating apparent K_d values from the constants; that is $K_d = k_{ads}/(k_{dsb} + k_{rem})$. The K_d's calculated in this way were either comparable with or greater than empirical K_d values. The situations in which the calculated K_d were greater than empirical were almost always the result of the value of k_{dsb} being found to be best fit at zero. If desorption is small, as the inversion suggests, then sinking of particulate Hg must be large enough to maintain particle concentrations at their observed values. Thus, our

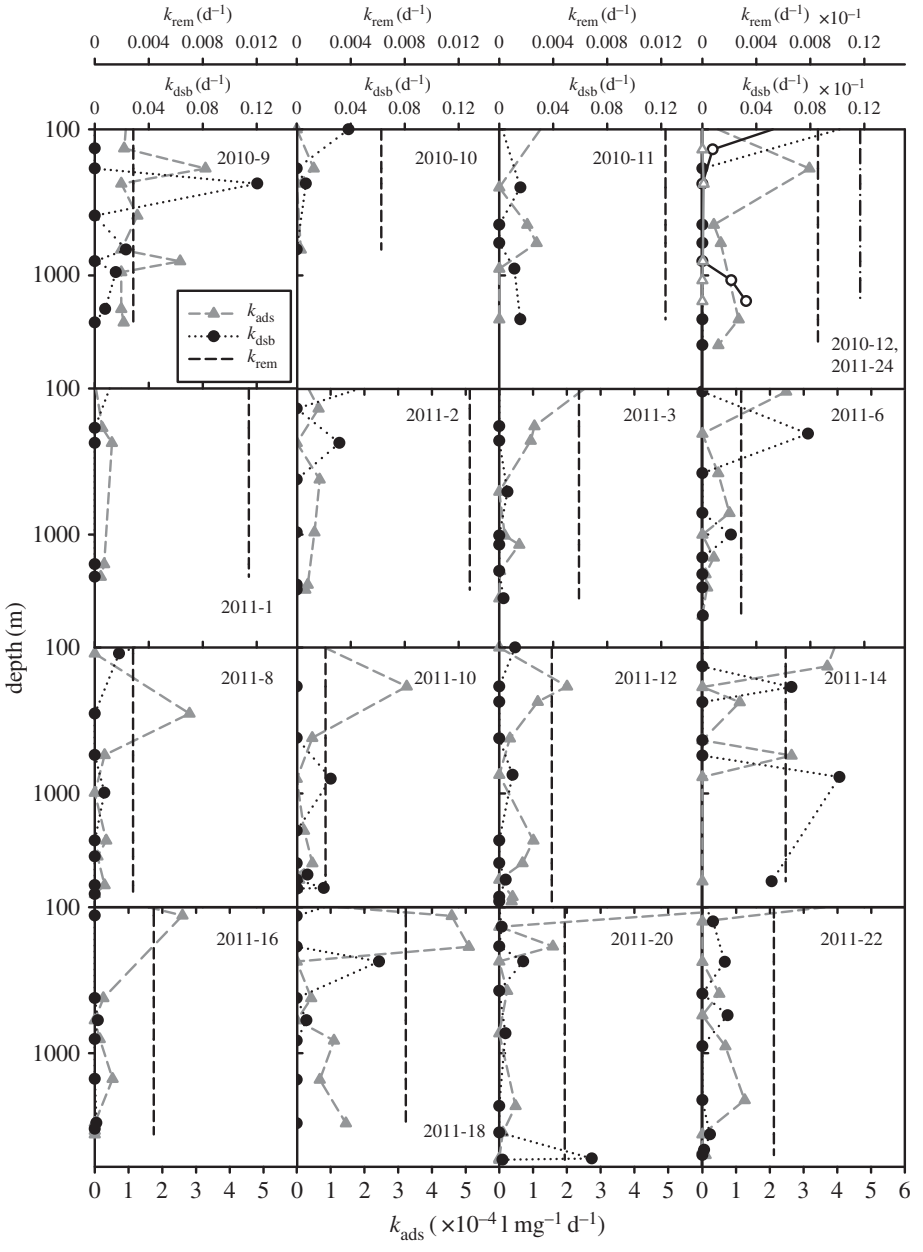

Figure 5. Station-by-station results from inversion of equation (3.5). The rate constant for Hg adsorption (k_{ads}) is shown in circles, for desorption (k_{dsb}) in triangles and for remineralization (k_{rem}) in dashed vertical lines. For the two stations that occupied the same location (2010-12 and 2011-24), the 2011 occupation is shown with open symbols and with the dot-dashed line.

inversion modelling suggests the best description of Hg particle dynamics is one of steady state between adsorption, remineralization and sinking, with little influence of desorption.

The residence time of Hg in dissolved and particle phases can be estimated from these inversion rate constants. The mean value for k_{ads} from deeper waters > 1000 m was about 10^{-4} l (µg d)$^{-1}$ and the average SPM at these depths was about 5 µg l^{-1}. Thus, the residence time of dissolved Hg with respect to scavenging is approximately 5 years in North Atlantic water deeper than approximately 1000 m. The average k_{rem} was approximately 7×10^{-3} d^{-1}, leading to

an estimated residence time of Hg in the particle phase of approximately 0.4 years. The residence time of all forms of Hg in the deep ocean with respect to scavenging to sediments can also be estimated from our observed dissolved/particle partitioning:

$$\tau \approx \frac{\text{depth}[\text{Hg}_{\text{diss}}]}{w[\text{Hg}_{\text{part}}]} = \frac{\text{depth}[\text{Hg}_{\text{diss}}]}{wK_{\text{d}}[\text{SPM}][\text{Hg}_{\text{diss}}]} = \frac{\text{depth}}{wK_{\text{d}}[\text{SPM}]} \tag{3.6}$$

and is about 20–3200 years when height above the seafloor is taken to be 3000 m (the depth of the deep ocean if it is taken to be 1000–4000 m). As mixing time of water as a result of thermohaline circulation is about 1000 years, this may be consistent with our earlier observation that Hg in the deep ocean increases in a nutrient-like way [9,10]. The mean K_{d} value ($10^{6.65}\,1\,\text{kg}^{-1}$), however, suggests a relatively short residence time of only about 180 years, which would be inconsistent with deep-water Hg concentration trends across basins. Further research is needed to resolve this inconsistency including the measurement of Hg fluxes in the deep sea and examination of the Hg distribution between small- and large-sized particles.

4. Conclusion

We found, through examination of our North Atlantic GEOTRACES measurements, that the particle cycling dynamics of Hg are different in potentially significant ways than has been previously assumed. For example, we found K_{d} values of Hg to be greater than conventionally used, but that assumptions of relatively uniform vertical and basin-wide distributions were good approximations. These observations in the North Atlantic remain to be tested in other parts of the ocean, however. The relatively high K_{d} values appear to be supported by a balance between adsorption of dissolved Hg, remineralization of the particle substrate and loss from the water column by sinking. Surprisingly, desorption of Hg from the particle phase to solution did not appear necessary to explain Hg species distributions, suggesting a model of Hg particle cycling that is perhaps better described as 'regenerative scavenging' rather than 'reversible scavenging'. Finally, the components of marine particles that most influence the sorption of Hg may not only be the organic matter, long thought to be dominant, but also calcium carbonate. This finding, as well as the suggestion that other phases such as biogenic silica and lithogenic material are unimportant, suggests that Hg scavenging and associated particle cycling may be region- and time-dependent as the dominant materials in marine particles change as a result of local biogeochemistry and ecosystem structure. Such dependencies could be included in models of Hg biogeochemistry to see if they offer refinements in our understanding of Hg cycling and make specific predictions about the cycling of this toxic metal for the future.

Data accessibility. The data from this work are accessible through BCO-DMO and the GEOTRACES Intermediate Data Product.

Authors' contributions. C.H.L., C.R.H. and K.L.B. all contributed to the writing of the manuscript, went on the cruises and did the analyses.

Competing interests. The authors declare to have no competing interests.

Funding. This work was supported by the US National Science Foundation through grants to C.H.L. and C.R.H.: OCE-1132515, OCE-0928191, OCE-1132480, OCE-0927274, OCE-1232760, OCE-1232979, OCE-1534315, OCE-1434653 and OCE-1434650. We thank Don Rice and Simone Metz for their support of the US GEOTRACES program.

Acknowledgements. We thank Phoebe Lam for aiding in data processing, Yanxu Zhang for discussions of Hg ocean modelling and Seth John for discussions regarding particle modelling. We are also grateful for the very helpful comments of two anonymous reviewers.

References

1. Jensen S, Jernelöv A. 1969 Biological methylation of mercury in aquatic organisms. *Nature* **223**, 753–754. (doi:10.1038/223753a0)
2. Mason RP, Morel FMM, Hemond HF. 1995 The role of microorganisms in elemental mercury formation in natural waters. *Water Air Soil Pollut.* **80**, 775–787. (doi:10.1007/BF01189729)

3. Azam F. 1998 Microbial control of oceanic carbon flux: the plot thickens. *Science* **280**, 694–696. (doi:10.1126/science.280.5364.694)
4. Buesseler KO, Boyd PW. 2009 Shedding light on processes that control particle export and flux attenuation in the twilight zone of the open ocean. *Limnol. Oceanogr.* **54**, 1210–1232. (doi:10.4319/lo.2009.54.4.1210)
5. Steinberg DK, Van Mooy BAS, Buesseler KO, Boyd PW, Kobari T, Karl DM. 2008 Bacterial vs. zooplankton control of sinking particle flux in the ocean's twilight zone. *Limnol. Oceanogr.* **53**, 1327–1338. (doi:10.4319/lo.2008.53.4.1327)
6. Ducklow HW, Steinberg DK, Buesseler KO. 2001 Upper ocean carbon export and the biological pump. *Oceanography* **14**, 50–58. (doi:10.5670/oceanog.2001.06)
7. Honda MC, Imai K, Nojiri Y, Hoshi F, Sugawara T, Kusakabe M. 2002 The biological pump in the northwestern North Pacific based on fluxes and major components of particulate matter obtained by sediment-trap experiments (1997–2000). *Deep-Sea Res. II Top. Stud. Oceanogr.* **49**, 5595–5625. (doi:10.1016/S0967-0645(02)00201-1)
8. Lamborg C, Bowman K, Hammerschmidt C, Gilmour C, Munson K, Selin N, Tseng C-M. 2014 Mercury in the anthropocene ocean. *Oceanography* **27**, 76–87. (doi:10.5670/oceanog.2014.11)
9. Zhang Y, Jaeglé L, Thompson L. 2014 Natural biogeochemical cycle of mercury in a global three-dimensional ocean tracer model. *Glob. Biogeochem. Cycles* **28**, GB004814. (doi:10.1002/2014GB004814)
10. Lamborg CH *et al.* 2014 A global ocean inventory of anthropogenic mercury based on water column measurements. *Nature* **512**, 65–68. (doi:10.1038/nature13563)
11. Strode S, Jaegle L, Emerson S. 2010 Vertical transport of anthropogenic mercury in the ocean. *Glob. Biogeochem. Cycles* **24**, GB003728. (doi:Gb4014/10.1029/2009GB003728)
12. Mason RP, Rolfhus KR, Fitzgerald WF. 1998 Mercury in the North Atlantic. *Mar. Chem.* **61**, 37–53. (doi:10.1016/S0304-4203(98)00006-1)
13. Ravichandran M. 2004 Interactions between mercury and dissolved organic matter—a review. *Chemosphere* **55**, 319–331. (doi:10.1016/j.chemosphere.2003.11.011)
14. Bowman KL, Hammerschmidt CR, Lamborg CH, Swarr G. 2015 Mercury in the North Atlantic Ocean: the U.S. GEOTRACES zonal and meridional sections. *Deep Sea Res. II Top. Stud. Oceanogr.* **116**, 251–261. (doi:10.1016/j.dsr2.2014.07.004)
15. Lam PJ, Ohnemus DC, Auro ME. 2015 Size-fractionated major particle composition and concentrations from the US GEOTRACES North Atlantic Zonal Transect. *Deep Sea Res. II Top. Stud. Oceanogr.* **116**, 303–320. (doi:10.1016/j.dsr2.2014.11.020)
16. Lamborg CH, Hammerschmidt CR, Gill GA, Mason RP, Gichuki S. 2012 An intercomparison of procedures for the determination of total mercury in seawater and recommendations regarding mercury speciation during GEOTRACES cruises. *Limnol. Oceanogr. Methods* **10**, 90–100. (doi:10.4319/lom.2012.10.90)
17. Cutter GA, Bruland KW. 2012 Rapid and noncontaminating sampling system for trace elements in global ocean surveys. *Limnol. Oceanogr. Methods* **10**, 425–436. (doi:10.4319/lom.2012.10.425)
18. Bruland KW, Rue EL, Smith GJ, DiTullio GR. 2005 Iron, macronutrients and diatom blooms in the Peru upwelling regime: brown and blue waters of Peru. *Mar. Chem.* **93**, 81–103. (doi:10.1016/j.marchem.2004.06.011)
19. Munson KM, Lamborg CH, Swarr GJ, Saito MA. 2015 Mercury species concentrations and fluxes in the central tropical Pacific Ocean. *Glob. Biogeochem. Cycles* **29**, 656–676. (doi:10.1002/2015GB005120)
20. Martin JH, Knauer GA, Karl DM, Broenkow WW. 1987 VERTEX: carbon cycling in the NE Pacific. *Deep-Sea Res.* **34**, 267–285. (doi:10.1016/0198-0149(87)90086-0)
21. Hayes CT *et al.* 2015 Intensity of Th and Pa scavenging partitioned by particle chemistry in the North Atlantic Ocean. *Mar. Chem.* **170**, 49–60. (doi:10.1016/j.marchem.2015.01.006)
22. Owens SA, Pike S, Buesseler KO. 2015 Thorium-234 as a tracer of particle dynamics and upper ocean export in the Atlantic Ocean. *Deep Sea Res. II Top. Stud. Oceanogr.* **116**, 42–59. (doi:10.1016/j.dsr2.2014.11.010)
23. Jenkins WJ, Smethie Jr WM, Boyle EA, Cutter GA. 2015 Water mass analysis for the U.S. GEOTRACES (GA03) North Atlantic sections. *Deep Sea Res. II Top. Stud. Oceanogr.* **116**, 6–20. (doi:10.1016/j.dsr2.2014.11.018)

24. Balcom PH, Hammerschmidt CR, Fitzgerald WF, Lamborg CH, O'Connor JS. 2008 Seasonal distributions and cycling of mercury and methylmercury in the waters of New York/New Jersey Harbor Estuary. *Mar. Chem.* **109**, 1–17. (doi:10.1016/j.marchem.2007.09.005)
25. Balcom PH, Fitzgerald WF, Vandal GM, Lamborg CH, Rolfhus KR, Langer CS, Hammerschmidt CR. 2004 Mercury sources and cycling in the Connecticut River and Long Island Sound. *Mar. Chem.* **90**, 53–74. (doi:10.1016/j.marchem.2004.02.020)
26. Luengen AC, Flegal AR. 2009 Role of phytoplankton in mercury cycling in the San Francisco Bay estuary. *Limnol. Oceanogr.* **54**, 23–40. (doi:10.4319/lo.2009.54.1.0023)
27. Hammerschmidt CR, Fitzgerald WF. 2006 Methylmercury cycling in sediments on the continental shelf of southern New England. *Geochim. Cosmochim. Acta* **70**, 918–930. (doi:10.1016/j.gca.2005.10.020)
28. Zhang Y, Jaeglé L, Thompson L, Streets DG. 2014 Six centuries of changing oceanic mercury. *Glob. Biogeochem. Cycles* **28**, GB004939. (doi:10.1002/2014GB004939)
29. Johannesson KH, Neumann K. 2013 Geochemical cycling of mercury in a deep, confined aquifer: insights from biogeochemical reactive transport modeling. *Geochim. Cosmochim. Acta* **106**, 25–43. (doi:10.1016/j.gca.2012.12.010)
30. Marchal O, Lam PJ. 2012 What can paired measurements of Th isotope activity and particle concentration tell us about particle cycling in the ocean? *Geochim. Cosmochim. Acta* **90**, 126–148. (doi:10.1016/j.gca.2012.05.009)
31. Murnane RJ, Cochran JK, Buesseler KO, Bacon MP. 1996 Least-squares estimates of thorium, particle, and nutrient cycling rate constants from the JGOFS North Atlantic Bloom Experiment. *Deep Sea Res. I Oceanogr. Res. Papers* **43**, 239–258. (doi:10.1016/0967-0637(96)00004-0)
32. Bacon MP, Anderson RF. 1982 Distribution of thorium isotopes between dissolved and particulate forms in the deep sea. *J. Geophys. Res.* **87**, 2045–2056. (doi:10.1029/JC087iC03p02045)
33. Clegg SL, Whitfield M. 1990 A generalized model for the scavenging of trace metals in the open ocean—I. Particle cycling. *Deep Sea Res.* **37**, 809–832. (doi:10.1016/0198-0149(90)90008-J)
34. John SG, Conway TM. 2014 A role for scavenging in the marine biogeochemical cycling of zinc and zinc isotopes. *Earth Planet. Sci. Lett.* **394**, 159–167. (doi:10.1016/j.epsl.2014.02.053)
35. Ledwell JR, Watson AJ, Law CS. 1993 Evidence for slow mixing across the pycnocline from an open-ocean tracer-release experiment. *Nature* **364**, 701–703. (doi:10.1038/364701a0)